

Behavior of hydrogen in wide band gap oxides

K. Xiong, J. Robertson, and S. J. Clark

Citation: *Journal of Applied Physics* **102**, 083710 (2007); doi: 10.1063/1.2798910

View online: <http://dx.doi.org/10.1063/1.2798910>

View Table of Contents: <http://scitation.aip.org/content/aip/journal/jap/102/8?ver=pdfcov>

Published by the [AIP Publishing](#)

Articles you may be interested in

[A pathway to p -type wide-band-gap semiconductors](#)

Appl. Phys. Lett. **95**, 172109 (2009); 10.1063/1.3247890

[Branch-point energies and band discontinuities of III-nitrides and III-II-oxides from quasiparticle band-structure calculations](#)

Appl. Phys. Lett. **94**, 012104 (2009); 10.1063/1.3059569

[High capacity oxide/ferroelectric/oxide stacks for on-chip charge storage](#)

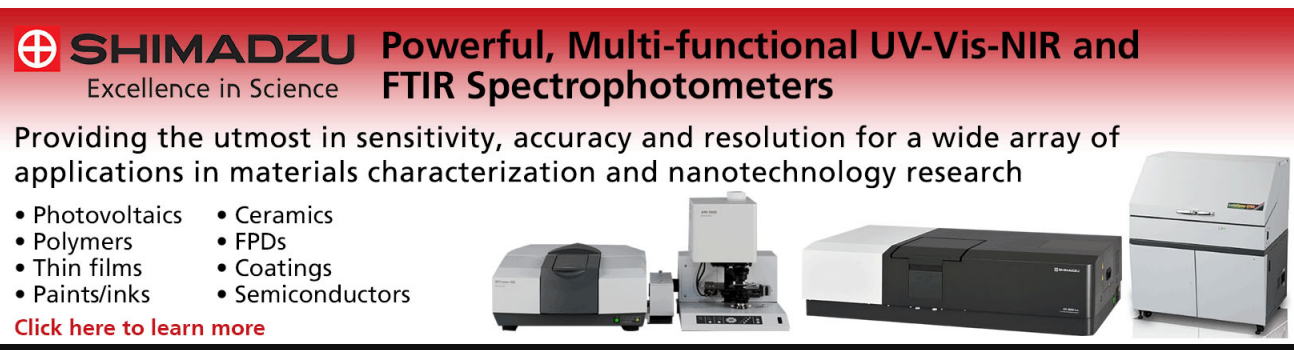
Appl. Phys. Lett. **89**, 042906 (2006); 10.1063/1.2236265

[Hydrogen-induced defects and degradation in oxide ferroelectrics](#)

Appl. Phys. Lett. **85**, 2577 (2004); 10.1063/1.1795975

[Band offsets of wide-band-gap oxides and implications for future electronic devices](#)

J. Vac. Sci. Technol. B **18**, 1785 (2000); 10.1116/1.591472

The advertisement features a red-to-white gradient background. On the left, the Shimadzu logo (a red circle with a white cross) is followed by the word 'SHIMADZU' in bold black letters, with 'Excellence in Science' in a smaller font below it. To the right of this, the text 'Powerful, Multi-functional UV-Vis-NIR and FTIR Spectrophotometers' is written in a large, bold, black font. Below this, a paragraph states: 'Providing the utmost in sensitivity, accuracy and resolution for a wide array of applications in materials characterization and nanotechnology research'. A bulleted list follows, with two columns of items: 'Photovoltaics', 'Polymers', 'Thin films', 'Paints/inks', 'Ceramics', 'FPDs', 'Coatings', and 'Semiconductors'. At the bottom left, a red link says 'Click here to learn more'. On the right side, four different models of Shimadzu spectrophotometers are shown in a row, ranging from a small benchtop unit to a large floor-standing cabinet model.

Behavior of hydrogen in wide band gap oxides

K. Xiong^{a)} and J. Robertson^{b)}*Engineering Department, Cambridge University, Cambridge CB2 1PZ, United Kingdom*

S. J. Clark

Physics Department, Durham University, Durham DH1 3LE, United Kingdom

(Received 9 January 2007; accepted 27 August 2007; published online 23 October 2007)

The energy levels of interstitial hydrogen in various wide band gap oxides are calculated using a density function based method that does not need a band gap correction. The positive charge state has a large stabilization energy due to the formation of an O–H bond. The hydrogen level is found to be shallow in CdO, ZrO₂, HfO₂, La₂O₃, LaAlO₃, SnO₂, TiO₂, SrTiO₃, PbTiO₃, and SrBi₂Ta₂O₉, but deep in MgO, Al₂O₃, SiO₂, ZrSiO₄, HfSiO₄, and SrZrO₃. It is borderline in SrO. The predictions are found to agree well with the experimental behavior of muonium in these oxides. © 2007 American Institute of Physics. [DOI: 10.1063/1.2798910]

I. INTRODUCTION

Hydrogen is a ubiquitous impurity in many solids and particularly in oxides. Interstitial hydrogen can act in two ways in the perfect oxide lattice.^{1–4} It can be an amphoteric impurity, giving rise to deep gap states with positive, neutral, and negative charge states, or it can form a shallow level at the conduction band edge and act as a donor. In a defective semiconductor, hydrogen often has beneficial effects in passivating defects by tying off dangling bond defects. However, in oxides, donor activity is deterring, as it causes a loss of activity or the presence of fixed charge. Here, we consider the behavior of hydrogen in three classes of oxides, the high dielectric constant oxides to be used as gate oxides, the ferroelectric oxides, and transparent conducting oxides. We then compare this to the behavior of hydrogen and muonium^{5,6} in semiconductors and consider overall models of the behavior.

High dielectric constant (*K*) oxides will replace SiO₂ as the gate dielectric in future complementary metal oxide semiconductor (CMOS) devices. The leading candidates are based on HfO₂.^{7–11} However, they introduce fixed charge and traps, and degrade device mobility compared to SiO₂ gate oxide. Hydrogen is introduced into high-*K* oxide devices during the post-deposition anneal. In addition, high-*K* gate oxides grown by atomic layer deposition with organometallic precursors or using water as the oxidant can contain residual hydrogen. Ionized hydrogen centers are therefore possible sources of positive fixed charge. Hydrogen may also contribute to bias instability,¹¹ based on its behavior in SiO₂.

Another critical application of oxides is in random-access memories. Perovskite-based oxides such as Pb(Zr, Ti)O₃ (PZT) and SrBi₂Ta₂O₉ (SBT) are being developed for nonvolatile ferroelectric random-access memories (FeRAMs).¹² In FeRAMs, hydrogen from the forming gas anneal can cause a loss of switchable polarization (fatigue) and higher leakage currents.^{13–15} This problem requires the use of diffusion barriers in real devices. It has been known

that hydrogen acts as a donor in BaTiO₃ (Ref. 16) as the H ionizes to H⁺ plus an electron. The H⁺ ion combines with an O²⁻ ion to form an OH⁻ ion whose dipole could pin ferroelectric domains from switching.¹⁷

Finally, there is increasing interest in transparent conducting oxides (TCOs) such as ZnO, SnO₂, and In₂O₃. For many years, TCOs were used as conductors in active matrix displays. Recently, the wider field of oxide-based electronics has opened up, once the high electron mobility and ease of processing of *n*-type TCOs was realized.¹⁸ At the same time, there is continuing development of ZnO as a wide gap semiconductor. ZnO is easily accidentally doped *n* type. This could be due to O vacancies or Zn interstitials, but interstitial hydrogen is also a donor.¹⁹ Thus, the role of hydrogen in TCOs is also of interest.

At a more fundamental level, Cox *et al.*^{5,6} have made extensive studies on whether muonium forms localized or delocalized levels in many semiconductors and oxides. Muonium acts chemically like H, but with a smaller mass. Thus, muonium spin resonance provides a unique experimental signature of whether the H level is deep or shallow.

This paper studies the behavior of interstitial hydrogen in various wide band gap oxides, extending our previous work^{3,20} in two ways. First, we find the atomic structure of H in a wide range of oxides with different oxygen coordinations. This allows us to see chemical trends, and test previous models.^{1–3} Second, previous calculations^{1–4} used the local density approximation (LDA) which underestimates the band gaps by 30%–50%—or 70% in the case of SnO₂. For bulk materials, this underestimate can be corrected empirically by an upward shift of the conduction bands.²¹ For defects, however, a localized resonant level could move into the gap, as the gap is opened. It is preferable to use more advanced methods which give a better band gap to check this behavior. Here, we present calculations of the energy levels using a density-functional-based method called the weighted density approximation (WDA).

II. COMPUTATIONAL METHODS

There are various methods that can give improved band gaps such as the GW approximation,²² B3LYP,²³ LDA+U,

^{a)}Present address: NXP Semiconductors, Kapeldreef, B3001 Leuven, Belgium.

^{b)}Electronic mail: jr@eng.cam.ac.uk

self-interaction correction, or screened exchange. The GW approximation is based on the quasiparticle formalism, which is similar to the Kohn-Sham formalism but uses a self-energy term to describe the exchange correlation of the electrons. It is the most accurate method to calculate the corrections and is widely used.^{24–26} However, it is computationally expensive. The B3YLP is a hybrid method combining the Hatree-Fock approximation and LDA. It has been carried out on some semiconductors and gives reasonable band gaps.^{27,28} B3YLP is generally implemented for a localized orbital basis set.

Here, we use the WDA (Refs. 29–33) because it is implemented for a plane wave basis and it has a lower computational cost than GW. In WDA, the exchange-correlation interaction is given by a Coulomb-like interaction between the electronic charge density and the exchange-correlation hole of the electrons,³¹

$$\varepsilon_{XC}^{WDA}(r) = \frac{1}{2} \int \frac{n(r)n_{XC}(r,r')}{|r-r'|} dr',$$

where ε_{XC}^{WDA} is the exchange-correlation energy density, n is the electronic charge density, and n_{XC} is the exchange-correlation hole. It is written in the same way as in Kohn-Sham density functional theory but the exchange correlation now depends on the density around r instead of the density at point r . n_{XC} obeys the sum rule in which its integral is normalized to 1. The factor $\frac{1}{2}$ prevents double counting.

A key point about WDA is that it is an energy functional in the DFT sense. It could be used in variational calculations of the total energy, while its energy eigenvalues more accurately resemble the one-electron excitation spectrum.

The WDA functional is less well tested than B3LYP or screened exchange. WDA was introduced by Alonso and Girifalco.²⁹ Hybertsen and Louie³⁰ tested it for Si and Ge. Rushton *et al.*³¹ significantly improved its implementation. The main advantage of WDA over, say, screened exchange is its lower computational cost as it can use ultrasoft pseudopotentials with a lower plane wave cutoff energy. WDA has been implemented in CASTEP.³²

Our calculations use the total energy plane wave pseudopotential code CASTEP.³⁴ The atoms are presented by Vanderbilt ultrasoft pseudopotentials.³⁵ A plane wave cutoff of 300 eV was used and four k points were generated in the Brillouin zone using Monkhorst-Pack method. The H states are quite localized, so that the calculations do not need very large supercells. We constructed supercells that contain 31–57 atoms for various oxides. The H atom is then placed in an arbitrary position near the center of the cell. We considered all three charge states, denoted as H^- , H^0 , and H^+ . The structures were relaxed in GGA to minimize the total energy, with no constraints except that the supercell size was fixed to the bulk GGA value.

Note that, although WDA is an energy functional, due to computational expense, in this paper the structures are relaxed to minimum energy using the generalized gradient approximation (GGA) of LDA, and the eigenvalues were then calculated on these structures by WDA.

TABLE I. Calculated minimum band gaps for the GGA and WDA methods in eV, compared to the experimental values (Refs. 36–40), plus the estimated +/- level of hydrogen.

Compound	Band gap			H +/- level (eV)
	GGA (eV)	WDA (eV)	Exp (eV)	
MgO	5.0	7.7	7.83	5.0
SrO	4.3	6.0	5.9	5.6
CdO	-0.51	2.9	0.85	4.0
SiO ₂	6	9.2	9	5.5
Al ₂ O ₃	6.5	9.3	8.8	5.5
SnO ₂	0.98	4.4	3.6	4.2
TiO ₂	2.0	2.7	3.06	4
<i>c</i> -ZrO ₂	3.4	6.0	5.8	6.0
<i>t</i> -ZrO ₂	4.3	6.2	...	6.2
<i>c</i> -HfO ₂	3.7	6.1	5.9	6.1
<i>t</i> -HfO ₂	4.3	6.4	...	6.4
ZrSiO ₄	4.7	7.0	6.5	4.5
HfSiO ₄	4.5	7.8	6.5–7	
La ₂ O ₃	3.7	6.9	5.7	6.4
Y ₂ O ₃	3.3	6.98	6	
LaAlO ₃	3.1	6.7	5.7	6.6
SrTiO ₃	1.9	3.1	3.2	3.2
SrZrO ₃	3.3	6.0	5.5	4.3
PbTiO ₃	1.7	2.0	3.4	3.4
SrBi ₂ Ta ₂ O ₉	1.7	5.7	4.3	4.3

III. RESULTS

The minimum band gaps of various oxides calculated in WDA (Ref. 32) are given in Table I, compared to the experimental values^{36–40} and those from GGA.^{41–43} The table shows that the band gaps are improved significantly compared to GGA. The WDA method gives good band gaps for MgO, SiO₂, Al₂O₃, TiO₂, ZrO₂, HfO₂, and SrTiO₃. It slightly overestimates the band gaps of La₂O₃, LaAlO₃, SrZrO₃, ZrSiO₄, HfSiO₄, and SrBi₂Ta₂O₉. Note that for some oxides, such as SnO₂ or CdO, GGA severely underestimates the gap, not just by 30%. However, for two cases, PbTiO₃ and SrBi₂Ta₂O₉, the WDA band gap still needs improvement, the reason for the disagreement is being studied.

Interstitial hydrogen has two basic types of behavior in all oxides. In one case, H forms deep gap states in all of its three charge states, H^- , H^0 , and H^+ . In the second case, H acts as a donor with the H^0 state lying at or above the conduction band edge. It is immediately clear when H^0 acts as a donor, as the atomic configurations of H^0 and H^+ are the same— H^0 ionizes to H^+ with the electron being delocalized in the oxide conduction band, and H^+ forms a single, strong O–H bond to an O site. On the other hand, if H^0 is deep, H acts as a traditional interstitial, forming some longer, weak bonds to more than one neighboring oxygen. The second indication is from the local density of states (DOS). A donor H^0 gives rise to a resonant state in the oxide conduction band (CB), whereas a deep H^0 gives a state in the band gap. In both cases, H^+ causes large rearrangements of the host lattice. H^+ has no electrons and it forms a single dative O–H bond to oxygen using the O $2p$ lone pair electrons.

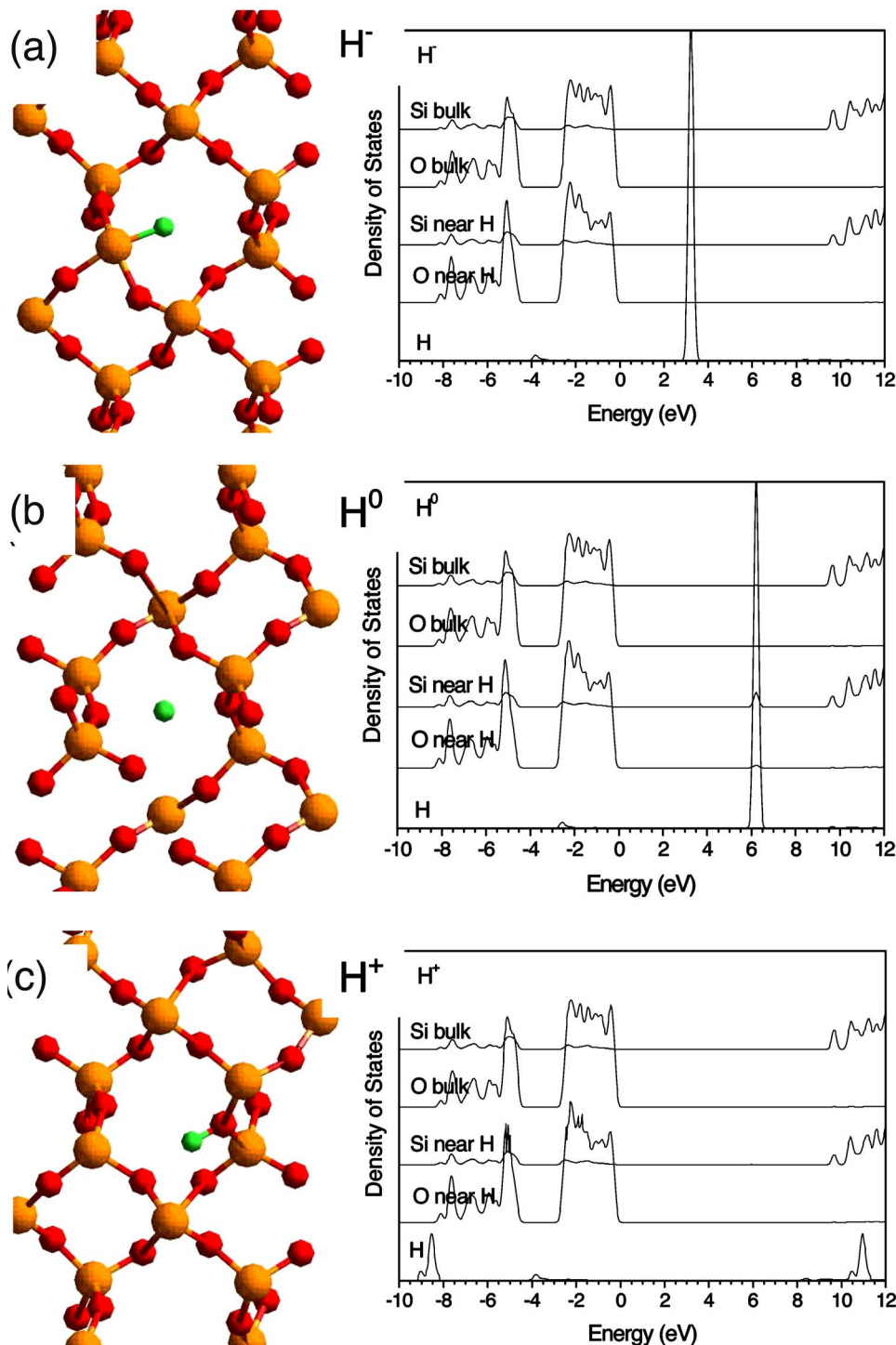


FIG. 1. (Color online) Calculated atomic configurations and WDA partial density of states of H in SiO₂: (a) H⁻, (b) H⁰, and (c) H⁺. Si in orange, O in red, and H in green.

A. SiO₂

Figures 1–4 show the relaxed atomic configurations and the calculated partial DOS for H in the *s-p* bonded oxides, MgO, SrO, CdO, SiO₂ and Al₂O₃. The bulk valence band maximum is set to 0 eV in all cases.

Consider first H in SiO₂. SiO₂ is the least polar of the oxides considered here; it has an open lattice with directional, covalent bonds and a very wide band gap of 9.0 eV. H is known to be deep in SiO₂.^{44,45} At H⁺, the H forms a short O–H bond of length of 0.98 Å to one host O atom. The oxygen becomes threefold coordinated in a pyramidal con-

figuration, Fig. 1(c). Unlike in other oxides, H does not need to break a host bond to form the O–H bond, because of the small O coordination number. The DOS in Fig. 1(c) shows that there is no gap state for H⁺ because the O–H bonding and antibonding states both lie in the bands. At the H⁰ site, the H forms an isolated interstitial site, Fig. 1(b), 2.0 Å away from other oxygens and it does not disturb the surrounding lattice. The DOS of H⁰ in Fig. 1(b) shows a defect state at 6.2 eV above the bulk valence band maximum (VBM). At the H⁻ site, the H forms a single bond of length of 1.55 Å to a positively charged Si site, Fig. 1(a). This makes the Si five-

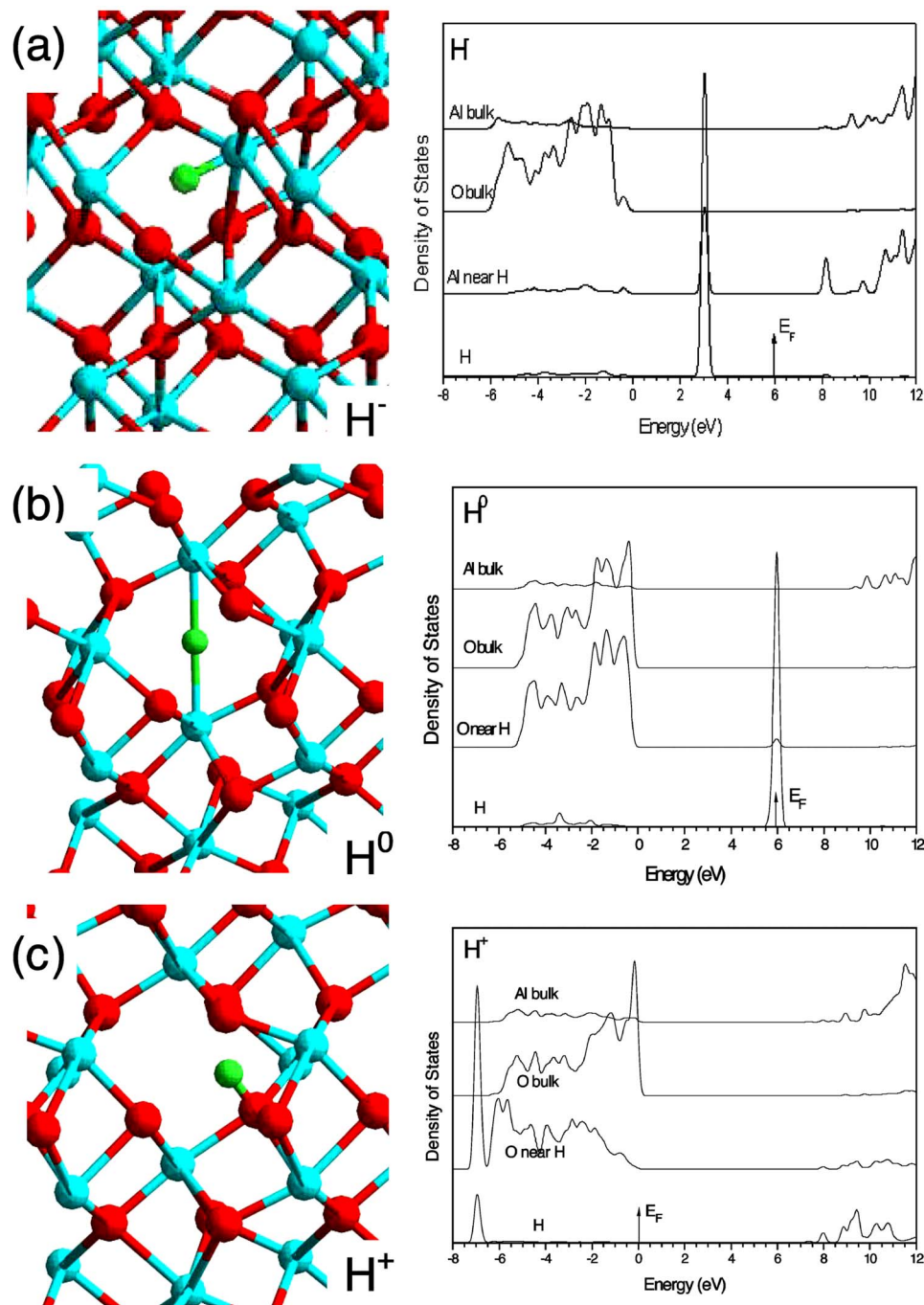


FIG. 2. (Color online) Calculated atomic configurations and WDA partial density of states of H in Al_2O_3 : (a) H^- , (b) H^0 , and (c) H^+ . Al in cyan, O in red, and H in green.

fold coordinated, and the Si–O bonds move away to accommodate the Si–H bond. The H^- level lies at 3.2 eV.

B. $\alpha\text{-Al}_2\text{O}_3$

Now consider H in $\alpha\text{-Al}_2\text{O}_3$ (sapphire). Al_2O_3 is more polar than SiO_2 . The Al is sixfold coordinated and O is fourfold coordinated. The atomic configuration of H^+ in Al_2O_3 [Fig. 2(a)] shows that the H^+ forms a O–H bond of length of 0.99 Å. The O breaks one of its Al–O bonds to accommodate the H^+ and remain fourfold coordinated. The DOS shows that there is no gap state for H^+ because the O–H bond and antibonding states lie in the bands. The sharp peak at -7 eV is due to O–H bonding states.

At H^0 , the interstitial H^0 does not bond to any host atom or cause its adjacent atoms to relax much from their initial

positions, Fig. 2(b). This is clear from the small variation of the Al–Al distance, about 0.08 Å. The H^0 creates a gap state at 6.0 eV above the VBM. At H^- , the H^- ion is attracted to an Al^{3+} ion forming a weak Al–H bond of length of 1.49 Å [Fig. 2(c)]. The distance between H^- and the three other adjacent Al^{3+} ions is ~ 3.0 Å. The Al^{3+} ion becomes fourfold coordinated, with three Al–O bonds and one Al–H bond. The Al–H group and the three O ions form a tetrahedron. The DOS shows that the H^- level lies at 3.0 eV.

C. MgO, SrO, and CdO

We next consider H in MgO, SrO, and CdO. These oxides have the rock salt structure, which is rather close

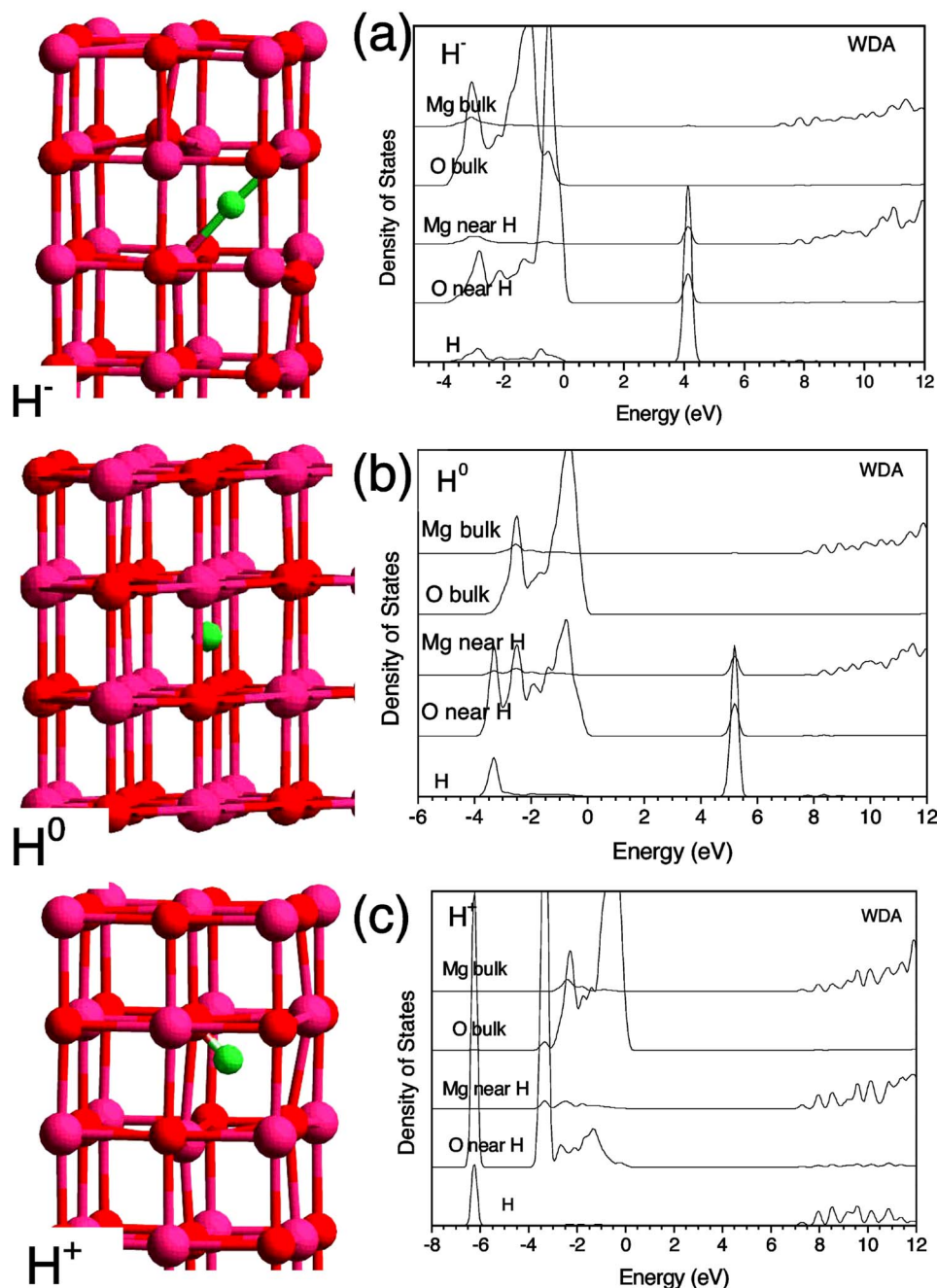


FIG. 3. (Color online) Calculated atomic configurations and WDA partial density of states of H in MgO: (a) H^- , (b) H^0 , and (c) H^+ . Mg in pink, O in red, and H in green.

packed. This makes the bonding of H atypical of other lattices. In MgO, H is deep. At H^+ , the H bonds to a host O^{2-} ion to form an OH^- ion. The O–H bond is 1.0 Å long and oriented along [110]. The lattice undergoes a large relaxation due to the positive charge of H, pushing the adjacent Mg^{2+} away, Fig. 3(c). The DOS has no defect state in the gap. At H^0 , the H lies in an interstitial position, away from both ion types. The H^0 level lies at 5.0 eV, Fig. 3(b). At H^- , the H lies near a Mg^{2+} ion and forms a weak Mg–H bond of length of 1.61 Å. The H^- level lies at 4.1 eV, Fig. 3(a).

SrO has a larger lattice constant and smaller band gap than MgO. H has all three charge states in the gap. However, the H^0 level lies very close to the conduction band edge, as seen by the peak at 6 eV in the partial density of states (PDOS) in Fig. 4(a), right. The O–H bond is fully formed for the H^0 state and is oriented along [110], Fig. 4(a), as for the

H^+ in MgO. H is showing some donorlike behavior. Thus, H in SrO is borderline between donor and deep. The Fermi energy is indicated by E_F in the PDOS.

CdO has a much narrower gap than SrO. CdO has an indirect gap, with a valence band maximum away from Γ .^{32,43} Experimentally, the minimum gap is about 0.8 eV and the smallest direct gap is 2.3 eV.³⁷ However, the minimum gap is negative in GGA. In WDA, it is 2.9 eV. We find that H behaves as a donor. The H^0 state is shown in Fig. 4(b). The H^0 has ionized to form H^+ . The O–H bond is oriented along [100] and is 0.98 Å long, pushing away the Cd^{2+} ion along this direction. The different orientation of H^+ probably arises because of the larger lattice constant of CdO, which allows the O–H bond to lie along [100], whereas in MgO, it was pushed along [110] because of lack of space. The PDOS

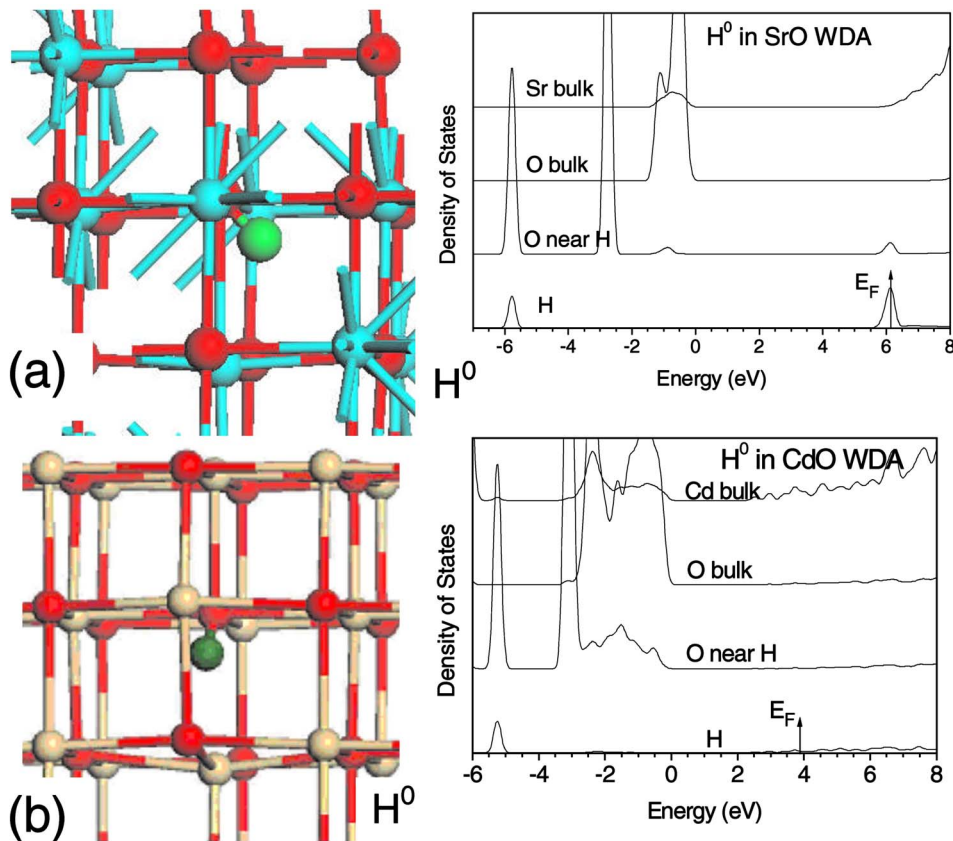


FIG. 4. (Color online) Calculated structure and WDA DOS of H^0 in (a) SrO, (b) CdO. Oxygen=red.

shows that the H state forms a broad resonance in the conduction band, Fig. 4(b).

The case of H in wurzite ZnO was previously studied in detail by van de Walle.¹⁹ H^0 is shallow, while H^+ must break a host Zn–O bond to form a O–H bond, leaving a fourfold coordinated O site.

D. SnO_2 and TiO_2

SnO_2 has the ionic rutile lattice with sixfold Sn sites and planar threefold O sites. Its minimum band gap is 3.6 eV, but it is badly underestimated in GGA at 0.9 eV. It is 4.4 eV in WDA. In SnO_2 , H^0 is found to be shallow. The H^+ ion forms an O–H bond of length of 0.98 Å normal to the Sn–O bonding plane, without the need to break a host Sn–O bond, as seen in Fig. 5. Indeed it barely disturbs the host lattice, because the donor is so delocalized. H^- acts similarly to H^0 .

We now turn to transition metal oxides. TiO_2 has the same rutile structure as SnO_2 . Its experimental band gap is 3.06 eV. Its gap in WDA is 2.7 eV, compared to 2.0 eV in GGA. H also acts as a shallow donor in TiO_2 . The H^+ site has the same structure as in SnO_2 , it is normal to the Ti–O bonding plane. H^- acts similarly to H^0 .

E. ZrO_2 and HfO_2

In cubic ZrO_2 , H acts as a donor. Zr is eightfold coordinated and O is fourfold coordinated. The H^+ bonds to an O^{2-} ion to form an OH group, with an O–H bond length of 1.017 Å oriented along [001]. The formation of an OH^- ion pushes an adjacent Zr^{4+} ion away, so that the O can remain fourfold coordinated. Similarly, the H^0 bonds to an O^{2-} ion

to form an OH^- ion, as shown in Fig. 6(a). The calculated O–H bond length is 1.072 Å, larger than 0.97 Å of the free OH^- ion, showing that H is borderline deep. The formation of the OH^- ion indicates that H^0 acts as a donor. The oxygen is still fourfold coordinated, it forms three bonds with the Zr^{4+} ions and one with H^+ . The OH^- ion and its three bonded Zr ions form a flatten pyramid with the O–H bond at the apex. The PDOS in Fig. 6(b) shows that the H state is resonant with the conduction band. The H^- state was found to form a similar configuration to H^0 , it is not shown for brevity.

H in cubic HfO_2 acts as a donor, similar to H in ZrO_2 . The H^+ forms an O–H bond with a bond length of 1.0 Å. In

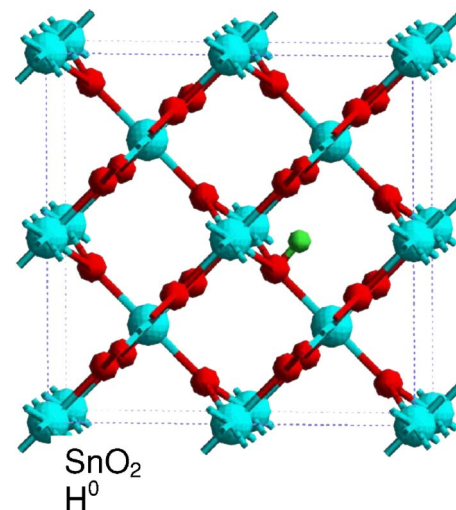


FIG. 5. (Color online) Calculated structure of H^+ in SnO_2 .

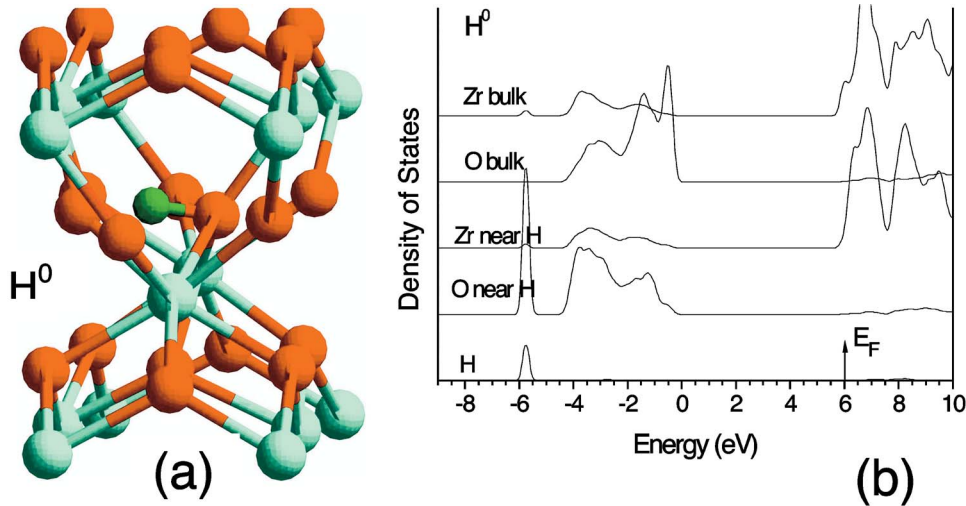


FIG. 6. (Color online) (a) Calculated atomic configurations of H^0 in cubic $ZrO_2:Zr$ in light blue, O in orange, and H in green. (b) WDA partial density of states of H^+ in cubic ZrO_2 .

contrast, for H^0 the O–H bond length is 0.99 Å, Fig. 7(a). The DOS shows that for H^0 there is no gap state, Fig. 7(b). The O–H bonding state at -6 eV confirms that the H^0 bonds strongly to O to form the OH ion.

We also consider H in tetragonal (t -) HfO_2 , which has a 0.3 eV wider band gap than cubic HfO_2 ,²⁵ as also seen in Table I. Nevertheless, H also acts as a donor in t - HfO_2 . Figure 7(c) shows the relaxed configuration of H^0 in t - HfO_2 . The structure undergoes a large relaxation. The formation of an O–H bond causes the Hf's bonded to the O to become planar. Therefore, unlike the H in c - HfO_2 , the OH group and

the three bonded Hf neighbors no longer form a flatten pyramid. The O–H bond length is 0.995 Å, oriented in (110). The PDOS in Fig. 7(d) shows that there is no gap state, so that the H^0 level lies in the CB. The H^- state forms a similar configuration to H^0 , it is not shown for brevity.

F. $ZrSiO_4$ and $HfSiO_4$

In the $ZrSiO_4$ crystal, the O is threefold coordinated, Zr eightfold, and Si fourfold. The Si–O bonding is covalent and the Zr–O bonding is ionic. The H^0 was found to stay in an

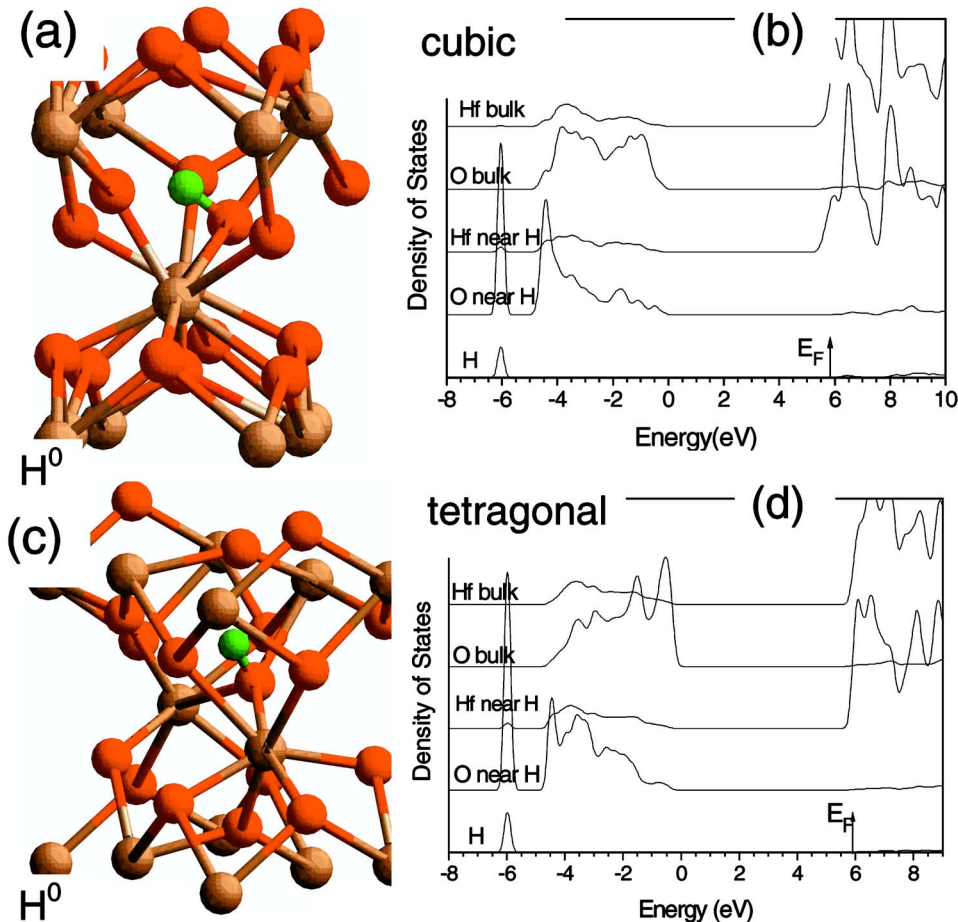


FIG. 7. (Color online) [(a) and (b)] Calculated atomic configurations and partial density of states of H^0 in cubic HfO_2 . [(c) and (d)] Calculated atomic configurations and partial density of states for H^0 in tetragonal HfO_2 . Hf in brown, O in orange, and H in green.

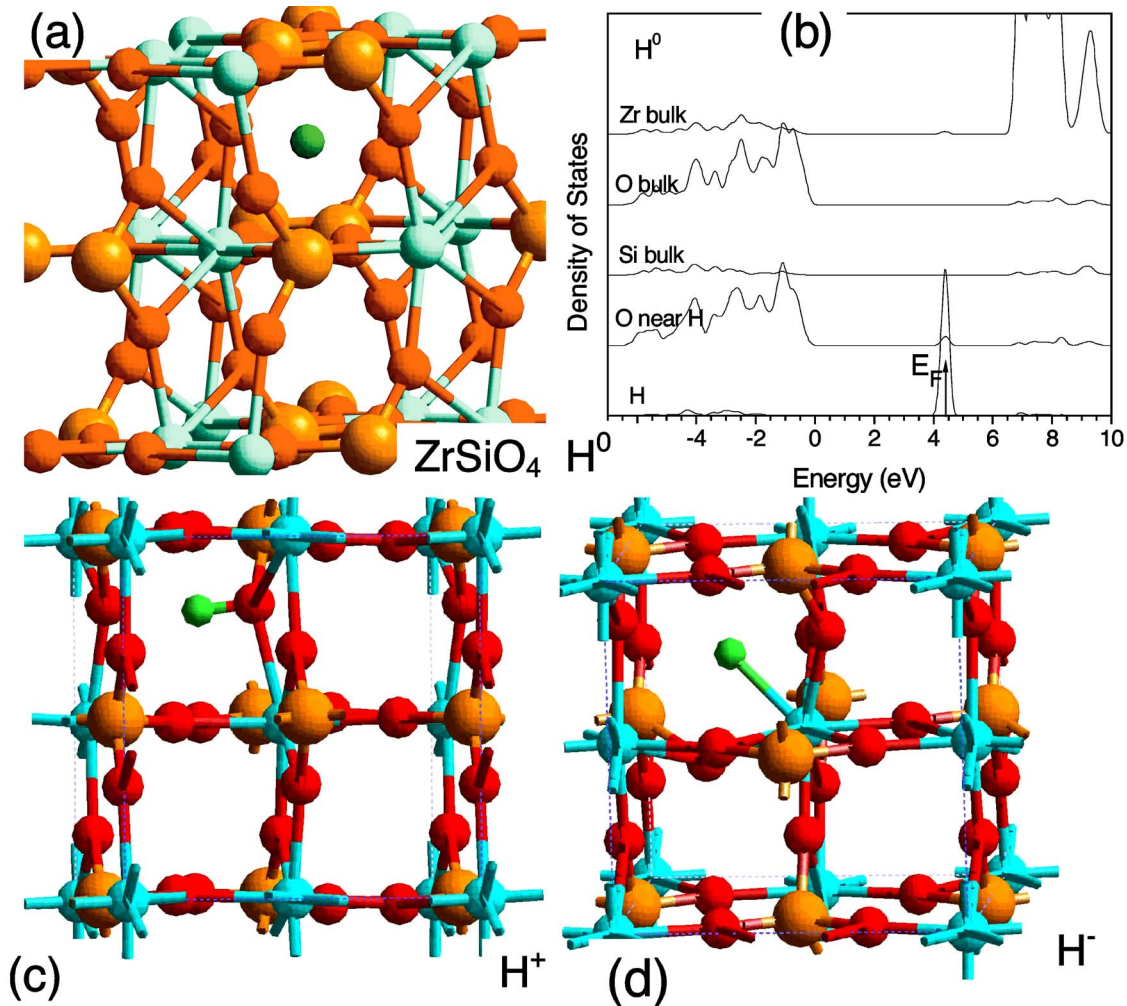


FIG. 8. (Color online) [(a) and (b)] Calculated atomic configurations and WDA partial density of states of H^0 in $ZrSiO_4$. [(c) and (d)] Atomic configurations of H^+ and H^- in $ZrSiO_4$, respectively. Zr=light blue, O=red, Si=orange, and H=green or white.

interstitial site within the plane that contains ZrO_2Si units, Fig. 8(a). The distance between the H^0 and its nearest oxygen neighbor is 1.893 Å. The DOS shows that H^0 forms a deep gap state at ~ 4.3 eV above the valence band top. Thus, H in $ZrSiO_4$ is deep, like in SiO_2 . The H^- state gives a deep level at 2.9 eV and the hydrogen bonds to the most electropositive species, Zr. At H^+ , the H^+ bonds to one oxygen, and pulls it out of the plane slightly to make a more tetrahedral configuration. H in $HfSiO_4$ behaves similar to $ZrSiO_4$.

G. La_2O_3

The atomic configuration of H^0 in La_2O_3 seen in Fig. 9(a) also shows the formation of the OH^- ion. It acts as a donor, but marginally. The O–H bond is oriented in (110) plane and is 0.977 Å long. It can be seen from the figure that the O is now bonded to three La neighbors. The DOS shows that the H^0 level in La_2O_3 lies 0.5 eV below the conduction band edge. It is borderline between deep and shallow. If the band gap is corrected from the WDA value of 6.9 eV to

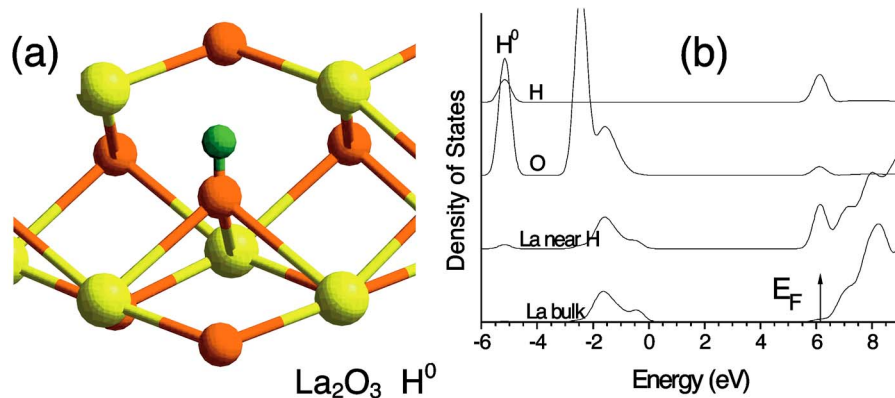


FIG. 9. (Color online) (a) Calculated atomic configurations of H^0 in La_2O_3 : La in yellow, O in red, and H in green. (b) WDA partial density of states of H^0 in La_2O_3 .

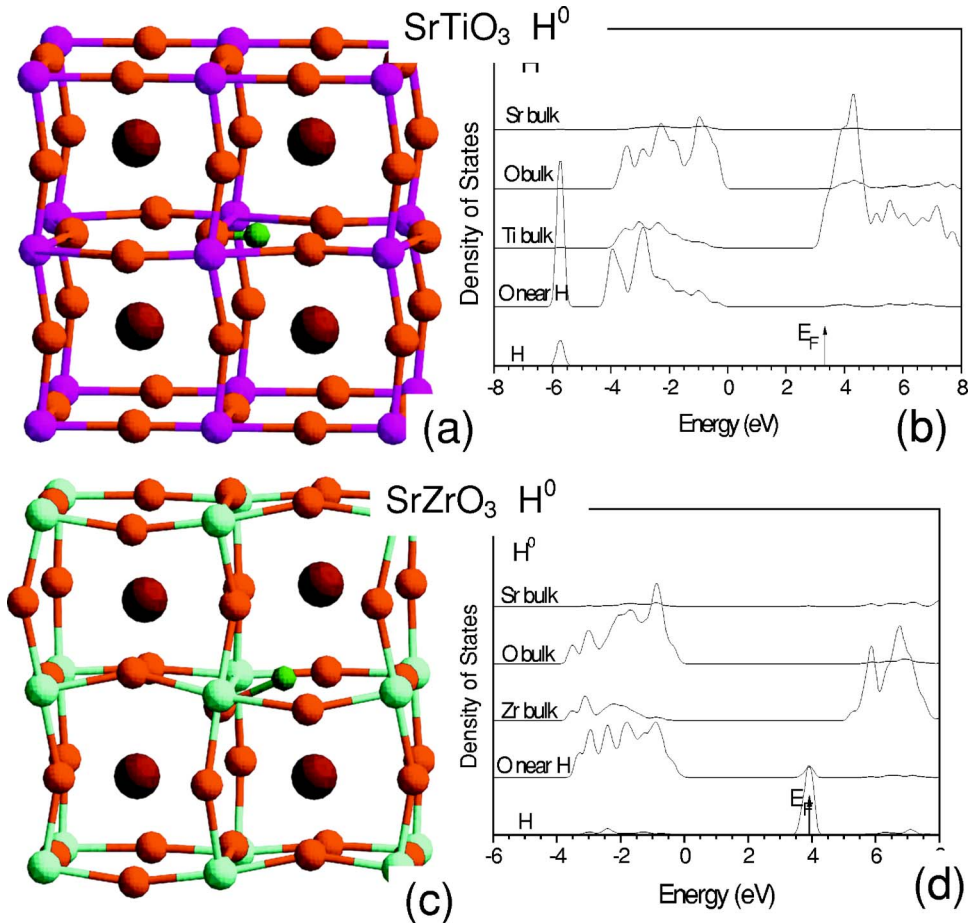


FIG. 10. (Color online) [(a) and (b)] Calculated atomic configurations and WDA partial density of states of H^0 in cubic $SrTiO_3$. [(c) and (d)] Calculated atomic configurations and WDA partial density of states of H^0 in $SrZrO_3$. Sr=dark red, Ti=purple, Zr=cyan, O=red, and H=green.

match the experimental band gap of 5.8 eV, the H^0 level lies at 5.4 eV above the VBM.

H. Perovskites

We next consider the behavior of H in perovskite oxides. The relaxed atomic structures for the H^0 in $SrTiO_3$ and $SrZrO_3$ are shown in Figs. 10(a) and 10(b), respectively. H is a shallow donor in $SrTiO_3$, as it is in $PbTiO_3$ but is deep in $SrZrO_3$.^{46,47}

For H^0 in $SrTiO_3$, the H forms a single short O–H bond to one O, Fig. 10(a). The DOS for the H^0 in $SrTiO_3$ [Fig.

10(b)] shows that the bonding state of the O–H bond of OH^- lies at -5.75 eV. The Fermi level lies at the bottom of the CB of $SrTiO_3$ and there are no gap states. This shows that the H forms a shallow donor level at the CB edge at 3.1 eV.

In contrast, H^0 in $SrZrO_3$ is weakly bonded to the O^{2-} ion, Fig. 10(c). The bond length is 1.7 Å, which is much longer than a free OH^- ion of 0.97 Å, indicating that the H^0 is deep and not ionized. H^0 in $SrZrO_3$ forms a deep state in the gap at 4.0 eV, Fig. 10(d).

We find that H is a donor in $LaAlO_3$. For H^0 , the H forms an OH^- ion of length of 1.026 Å oriented along [100],

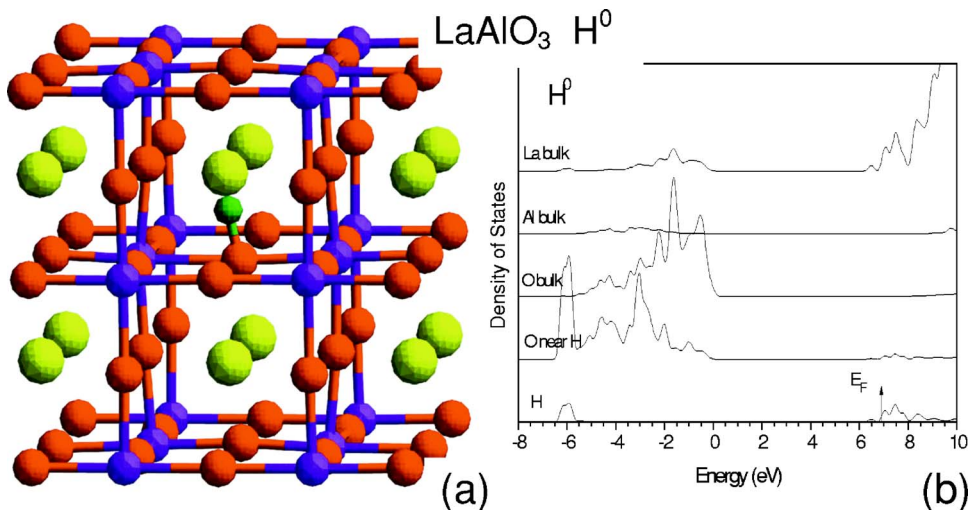


FIG. 11. (Color online) (a) Calculated atomic configurations of H^0 in $LaAlO_3$: La in yellow, Al in blue, O in red, and H in green. (b) WDA partial density of states of H^0 in $LaAlO_3$.

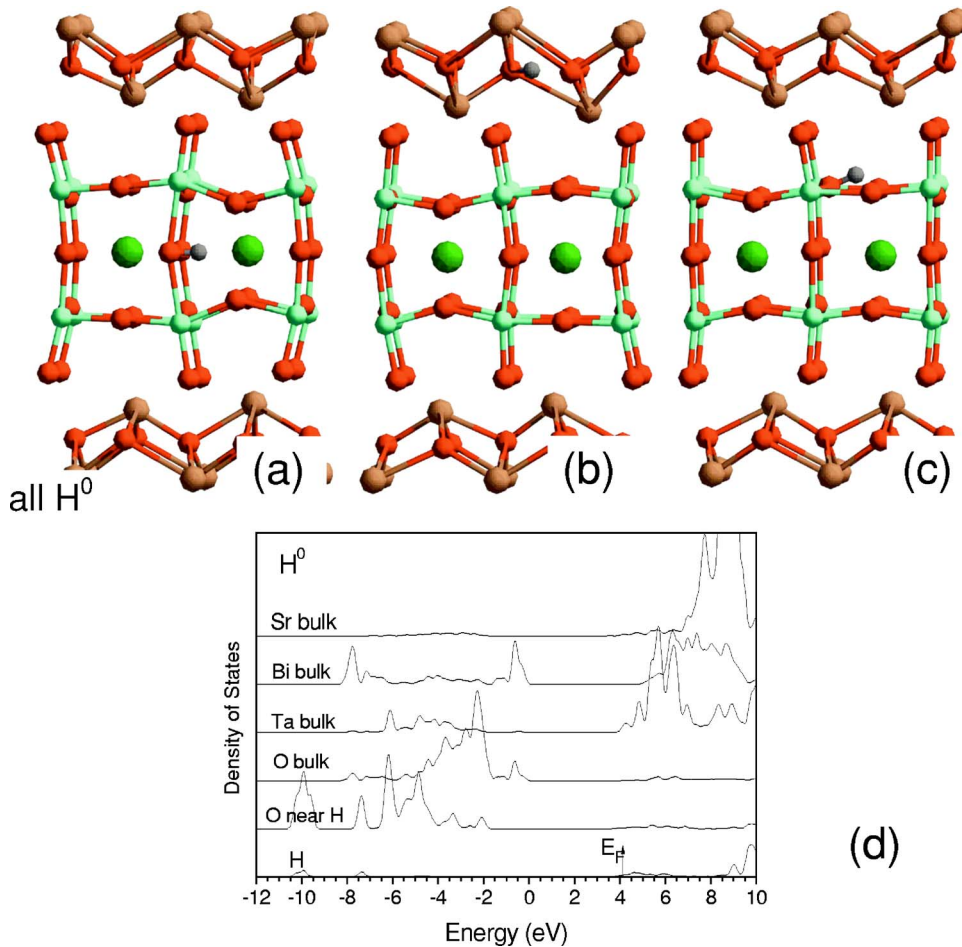


FIG. 12. (Color online) Calculated atomic configurations and WDA partial density of states of H^0 in $SrBi_2Ta_2O_9$. (a), (b), and (c) are the atomic configurations of H^0 in $SrBi_2Ta_2O_9$; Sr=green, Ta=light blue, O=red, and H=gray. (d) Partial density of states of H^0 in Bi_2O_2 block of SBT.

Fig. 11(a). The resulting OH^- ion pushes the two adjacent Al^{4+} ions away in opposite directions by about 0.1 \AA . The distortion indicates that the Al–O bonds around the OH^- are slightly weakened. The formation of the OH^- ion breaks inversion symmetry of the cubic phase. The H^0 level is in the CB at 6.9 eV , as seen in Fig. 11(b).

The layer perovskite SBT consists of TaO_3 perovskite block separated by a Bi_2O_2 layer. There are three places for an interstitial H in SBT, in the TaO_3 block, in the Bi_2O_2 layer, or in the intermediate region. The relaxed atomic configurations of H^0 in these three different layers are shown in Figs. 12(a)–12(c). We find that H^0 in SBT always acts as a donor. The calculated bond lengths are 0.97 , 0.979 , and 0.975 \AA for each case. All the O–H bonds have the same orientations. It was found that the most stable H^0 site is in the Bi_2O_2 layer, Fig. 12(b). It is 0.90 eV less stable in the TaO_3 block and 1.07 eV less stable in the intermediate layer. This result is useful because the ferroelectricity in SBT arises primarily from the Ta site displacements.⁴⁸ These are less affected if H prefers to be in the Bi_2O_2 layer.

These structures may be summarized as follows. The H^+ site shows a strong bonding of H to a lattice O^{2-} , in all oxides. This strongly stabilizes the H^+ configuration. If H acts as a donor, H^0 and H^- ionize to form H^+ . If H is deep, the H^0 site is basically nonbonded, while H^- is also weakly bonded, except in SiO_2 where there is some bonding to a bulk Si site.

IV. DISCUSSION

A. Relaxation and band gap correction

The formation energy $E(q)$ of the H interstitial is defined as the total energy of H in charge state q in the host $E(H, q)$ minus the energy of the bulk (E_{bulk}) of corresponding volume, the energy of hydrogen in the H_2 molecule,¹ and the energy of any charge,

$$E(q) = E_{\text{tot}}(H, q) - E_{\text{bulk}} - \frac{1}{2}E(H_2) + qE_F.$$

The last term accounts for the charge q supplied by a reservoir at the Fermi energy E_F .

Figure 13(a) shows the relative formation energy of H in SiO_2 in GGA plotted against E_F for its three charge states from Ref. 44. The electrical transition levels $E(q/q+1)$ is defined as the E_F at which the formation energy of the charge states q and $q+1$ is equal. In the absence of relaxation, or electron-electron repulsion, $E(0/-) \sim E(0/+)$. This is the case for H acting as a donor. However, if there is strong relaxation, as for H in SiO_2 , then $E(-/0)$ lies below $E(+/0)$ [Fig. 13(b)] and the relaxation energy is $U = E(0/+)-E(-/0)$.

However, GGA gives the wrong band gap. This paper calculated the eigenvalues $\varepsilon(q)$ of the gap state for each charge state in WDA, which gives close to the correct gap.

However, we do not have the WDA total energies or transition levels $E(q, q+1)$. To get these, we note that there can be strong relaxation for H^+ but not for H^0 or H^- . Thus, we can approximate, by Koopmans theorem, $E(0/-) = \frac{1}{2} [\varepsilon(0) + \varepsilon(-)]$ at the atomic positions of H^0 or H^- . We keep the same value of relaxation energy as in GGA, which is $[E(+/0) - E(0/-)]$. This allows us to find $E(+/0)$. The ultimate value of interest is $E(+/-)$, which is given by $E(+/-) = \frac{1}{2} [E(0/-) + E(+/0)]$, and this is tabulated for each oxide in Table I.

B. Models

A number of studies have been carried out of the behavior of hydrogen in semiconductors and oxides, and various models have been proposed. Kilic and Zunger¹ studied oxides and suggested that the H^0 level lay at a rather constant energy (~ 3.5 eV) below the vacuum level. In this model, H^0 is a donor if the oxide conduction band edge lies below 3.5 eV, that is, the electron affinity is more than 3.5 eV.

Van de Walle and Neugebauer² studied the tetrahedrally bonded AB semiconductors. They suggested that a 'universal' H^0 level lay close to the host's charge neutrality level (CNL). The argument is as follows. In binary AB semiconductors, the H^+ tends to bond to the anion and H^- tends to bond to the cation. However, to form an anion-H or cation-H bonds needs to break a host AB bond, leaving a cation or anion dangling bond (on the opposite species). Thus, the H^0 level will be located energetically midway between the anion dangling bond and cation dangling bond levels, which is the CNL of that material. The H^0 level would then tend to lie at a relatively constant energy when all the semiconductor band structures are aligned according to the experimental band offsets. In their model, H^0 would act as a donor if the universal H^0 level lay above its CB edge, that is, if the CNL lies above the CB edge.

Peacock and Robertson^{3,4} observed that, in high dielectric constant oxides, the H^+ tends to make a dative bond with an oxygen to form an OH^- ion. Therefore, unlike H in tetrahedral semiconductors, no cation-O bond is broken. This means that the H^+ level is essentially an O-H antibonding level. At H^- , H would break a metal-O bond to form a metal-H bond, leaving an oxygen dangling bond. Thus, the H^0 level lies at the average between the oxygen dangling bond and the O-H antibonding energies. Since the upper valence band of oxides consists of O $p\pi$ states, and the O-H antibonding level lies at a constant energy above the O 2p state (being solely dependent on the O-H bond length), the H^0 level will lie at a relatively constant energy above the oxide VB edge. Thus, H will act as a donor if the CB edge lies below some critical energy above VB—if the band gap is less than a critical value.

These three models give slightly different predictions. The vacuum level only appears in the model of Kilic and Zunger,¹ whereas the others depend only on the bulk bands. To an extent, they are not directly comparable, because the Van de Walle-Neugebauer² model refers to tetrahedral hosts, where H must break host bonds, whereas the oxides have a range of stoichiometries and H need not break a host bond.

The processes can perhaps best be understood using a general but easily understood model of Cox,^{6,49,50} in Fig. 14. The total energy of electrons in the H^0 and H^- level is taken as Δ_1 and Δ_2 above the VBM. The energy of electrons in the O-H bonding state of the OH^- ion is Δ_3 below the VBM, all taken as positive. E_0 is the energy of the host. The band gap is E_g . This allows us to define $E(+)=E_0-2\Delta_3$, $E(0)=E_0+\Delta_1$, and $E(-)=E_0+2\Delta_2$. Hence, we find

$$E(+/0) = \Delta_1 + 2\Delta_3,$$

$$E(0/-) = 2\Delta_2 - \Delta_1,$$

$$E(+/-) = 2(\Delta_2 + \Delta_3),$$

and thus

$$U = 2(\Delta_2 - \Delta_1 - \Delta_3).$$

The energy of the donor state is

$$E = E(+) + E_g.$$

The condition for shallow donors is then $E(+/-) > E_g$ or

$$\Delta_2 + \Delta_3 > E_g,$$

meaning that donor action occurs if the band gap is less than some value. This *band gap criterion* is closest to that of Peacock and Robertson.³

C. Comparison with experiment

The calculated $H^{+/-}$ levels for various oxides in WDA is summarized in Fig. 15(a). The energies are aligned at the top of the oxide valence bands. The calculated $H^{+/-}$ level is shallow in CdO, HfO₂, ZrO₂, La₂O₃, SrTiO₃, and LaAlO₃, while it is deep in MgO, SrO, SiO₂, Al₂O₃, and ZrSiO₄. For the oxides in which H acts as a shallow donor such as La₂O₃, we deduced that the H^0 level is placed 0.5 eV below the conduction band edge. In contrast, for SiO₂, Al₂O₃, MgO, ZrSiO₄, and SrZrO₃, the H^0 level lies above the valence band at 5.5, 5.5, 5, 4.5, and 4.4 eV. The calculated H^0 level in SiO₂ is higher than that calculated in LDA, and in MgO, it is lower than that found by Kilic and Zunger.¹ The $+/0$ level is at a reasonably constant energy with respect to the VB edge, as noted by Peacock and Robertson.³ The $+/-$ levels are not at a particularly constant energy below the vacuum level.

If the oxide bands are aligned to the Si bands by using the calculated band offsets^{9,51,52} as in Fig. 15(b), it can be seen that the $H^{+/-}$ level lies very close to or above the Si conduction band for HfO₂, ZrO₂, La₂O₃, LaAlO₃, SnO₂, and SrTiO₃. This indicates that H would act as a donor and release its electron to the Si channel. For MgO, Al₂O₃, and ZrSiO₄, the $H^{+/-}$ level lies deep or below the Si band gap. In these oxides, the H^0 could trap electrons from Si channel to form H^- , which is another stable charge state. We see that the $+/-$ level does not lie at a particularly constant level with respect to this energy scale, as was found by van de Walle and Neugebauer² for the tetrahedral semiconductors. In that model, the $+/-$ level lay at the CNL energy, and, in fact, it would allow a measurement of it. However, this model does not generalize as well to the oxides. This is because of the

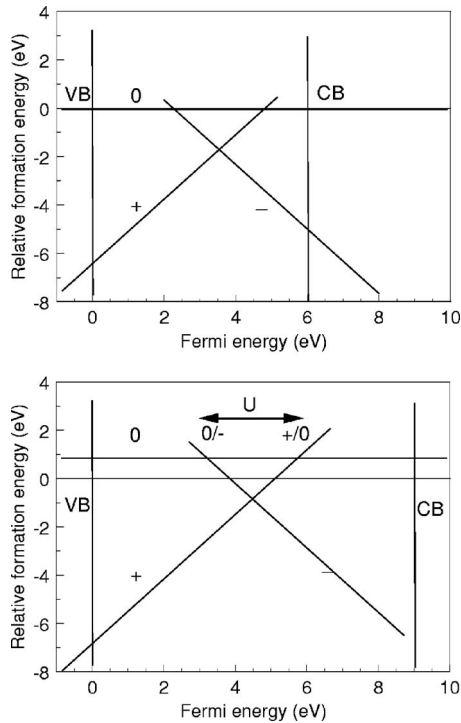


FIG. 13. Relative formation energy of H vs Fermi energy in SiO_2 : (a) uncorrected GGA result and (b) result corrected using WDA eigenvalues. Showing the relaxation energy U .

lower O coordination which means that formation of an O–H bond does not require the breaking of the metal–O bond, as it did in the tetrahedral semiconductors.

The hydrogen defect centers in semiconductors and oxides are very difficult to test because hydrogen possesses a high mobility and it tends to pair with other defects or impurities. However, its behavior can be compared to that of muonium. Muonium is easier to detect and it gives a different spin resonance decay spectrum if it forms a shallow or deep center. Cox *et al.*^{5,6} found that a trapped-atom Mu^0 state in SiO_2 , Al_2O_3 , and MgO and observed or inferred shallow Mu^+ states in CdO , SnO_2 , TiO_2 , ZrO_2 , HfO_2 , and La_2O_3 . They found that the shallow/deep behavior correlates closely with the *oxide band gap*. These experimental results are consistent with our theoretical predictions. Jennison *et al.*⁵³ suggested a stable H^- center in Al_2O_3 consistent with H being deep.

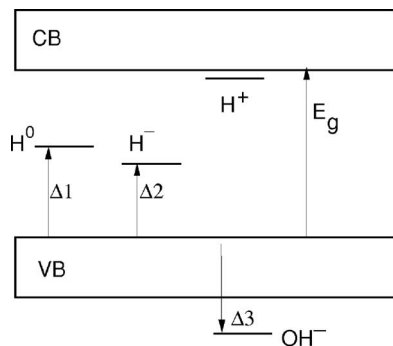


FIG. 14. Schematic energy levels of H^0 , H^- , and H^+ with ionized electron, according to the model of Cox *et al.* (Ref. 6).

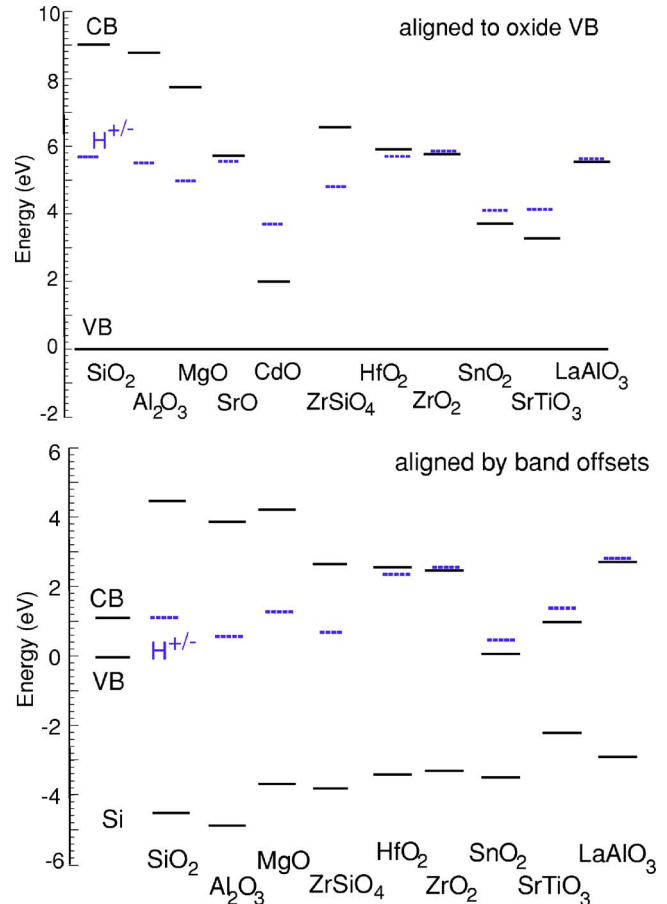


FIG. 15. (Color online) (a) Hydrogen $+/-$ energy levels in various oxides, aligned against the oxide valence band edge. (b) Hydrogen $+/-$ energy levels aligned according to the oxide band lineups.

V. CONCLUSIONS

First principles calculations of hydrogen-induced defect energy levels in various oxides were presented using a density functional method which does not need a band gap correction. Hydrogen was found to act as a shallow donor in ZrO_2 , HfO_2 , La_2O_3 , LaAlO_3 , SrTiO_3 , SBT , CdO , SnO_2 , and TiO_2 , but to give a deep state in Al_2O_3 , MgO , ZrSiO_4 , HfSiO_4 , SrZrO_3 , and SiO_2 . The results confirm the model that is proposed by Peacock and Robertson,³ that is, in oxides the $+/-$ level lies at a relatively constant energy above the top of the valence band.

ACKNOWLEDGMENT

The authors thank S. Cox for useful discussions.

- ¹C. Kilic and A. Zunger, Appl. Phys. Lett. **81**, 73 (2002).
- ²C. G. van de Walle and J. Neugebauer, Nature (London) **423**, 626 (2003).
- ³P. W. Peacock and J. Robertson, Appl. Phys. Lett. **83**, 2025 (2003).
- ⁴J. Robertson and P. W. Peacock, Thin Solid Films **445**, 155 (2003).
- ⁵S. F. J. Cox, J. Phys.: Condens. Matter **15**, 1727 (2003).
- ⁶S. F. J. Cox, J. L. Gavartin, J. S. Lord, S. P. Cottrell, J. M. Gil, H. V. Alberto, J. P. Duarte, R. C. Vilao, N. A. Campos, D. J. Keeble, E. A. Davis, M. Charlton, and D. P. van der Werf, J. Phys.: Condens. Matter **18**, 1079 (2006).
- ⁷G. Wilk, R. M. Wallace, and J. M. Anthony, J. Appl. Phys. **89**, 5243 (2001).
- ⁸J. Robertson, Eur. Phys. J.: Appl. Phys. **28**, 265 (2004).
- ⁹J. Robertson, J. Vac. Sci. Technol. B **18**, 1785 (2000).

- ¹⁰E. P. Gusev, D. A. Buchanan, E. Cartier, A. Kumar, S. Guha, A. Callegari, S. Zafar, P. C. Jamison, D. A. Neumayer, M. Copel, M. A. Gribelyuk, H. Okorn-Schmidt, C. D'Emic, P. Kozlowski, K. Chan, N. Bojarczuk, L. A. Ragnarsson, P. Ronsheim, K. Rim, R. J. Fleming, A. Mocuta, and A. Ajmera, *Tech. Dig. - Int. Electron Devices Meet.* **2001**, 455.
- ¹¹M. Houssa, L. Pantisano, L. A. Ragnarsson, R. Degraeve, T. Schram, G. Pourtois, S. DeGendt, G. Groesenken, and M. M. Heyns, *Mater. Sci. Eng.*, **R. 51**, 37 (2006).
- ¹²U. Bottger and S. R. Summerfelt, in *Nanoelectronics and Information Technology*, edited by R. Waser (Wiley, New York, 2003).
- ¹³Y. Shimamoto, K. Kushida-Abdelghafar, H. Miki, and Y. Fujisaki, *Appl. Phys. Lett.* **70**, 3096 (1997).
- ¹⁴J. P. Han and T. P. Ma, *Appl. Phys. Lett.* **71**, 1267 (1997).
- ¹⁵S. Zafar, V. Kaushik, P. Laberge, P. Chu, R. E. Jones, R. L. Hance, P. Zurcher, B. E. White, D. Taylot, B. Melnick, and S. Gillespie, *J. Appl. Phys.* **82**, 4469 (1997).
- ¹⁶R. Waser, *J. Am. Ceram. Soc.* **71**, 58 (1999).
- ¹⁷D. Dimos, W. L. Warren, M. B. Sinclair, B. A. Tuttle, and R. W. Schwartz, *J. Appl. Phys.* **76**, 4305 (1994).
- ¹⁸H. Hosono, *J. Non-Cryst. Solids* **352**, 851 (2006).
- ¹⁹C. G. van de Walle, *Phys. Rev. Lett.* **85**, 1012 (2000).
- ²⁰J. Robertson, K. Xiong, and S. J. Clark, *Thin Solid Films* **496**, 1 (2006).
- ²¹R. W. Godby, M. Schluter, and L. J. Sham, *Phys. Rev. Lett.* **56**, 2415 (1986).
- ²²M. S. Hybertsen and S. G. Louie, *Phys. Rev. B* **34**, 5390 (1986).
- ²³A. D. Becke, *J. Chem. Phys.* **98**, 5648 (1993).
- ²⁴F. Aryasetiawan and O. Gunnarsson, *Rep. Prog. Phys.* **51**, 2327 (1998).
- ²⁵B. Kralik, E. K. Chang, and S. G. Louie, *Phys. Rev. B* **57**, 7027 (1998).
- ²⁶J. Dabrowski, V. Zavadinsky, and A. Fleszar, *Microelectron. Reliab.* **41**, 1093 (2001).
- ²⁷J. Muscat, A. Wander, and N. M. Harrison, *Chem. Phys. Lett.* **342**, 397 (2001).
- ²⁸J. Robertson, P. W. Peacock, M. D. Towler, and R. Needs, *Thin Solid Films* **411**, 96 (2002).
- ²⁹J. A. Alonso and L. A. Girifalco, *Phys. Rev. B* **17**, 3735 (1976).
- ³⁰M. S. Hybertsen and S. G. Louie, *Phys. Rev. B* **30**, 5777 (1984).
- ³¹P. P. Rushton, D. J. Tozer, and S. J. Clark, *Phys. Rev. B* **65**, 235203 (2002).
- ³²J. Robertson, K. Xiong, and S. J. Clark, *Phys. Status Solidi B* **243**, 2054 (2006).
- ³³K. Xiong, J. Robertson, M. C. Gibson, and S. J. Clark, *Appl. Phys. Lett.* **87**, 062105 (2005).
- ³⁴M. D. Segall, P. J. D. Lindan, M. J. Probert, C. J. Pickard, P. J. Hasnip, S. J. Clark, and M. C. Payne, *J. Phys.: Condens. Matter* **14**, 2717 (2002).
- ³⁵D. Vanderbilt, *Phys. Rev. B* **41**, 7892 (1990).
- ³⁶A. S. Rao and R. J. Kearney, *Phys. Status Solidi B* **95**, 243 (1979).
- ³⁷P. Koffyberg, *Phys. Rev. B* **13**, 4470 (1976).
- ³⁸R. C. Whited, C. J. Flaten, and W. C. Walker, *Solid State Commun.* **13**, 1903 (1973).
- ³⁹R. H. French, *J. Am. Ceram. Soc.* **73**, 477 (1990).
- ⁴⁰Z. M. Jarzebksi, *J. Electrochem. Soc.* **123**, 299 (1976).
- ⁴¹O. E. Taurian, M. Springborg, and N. E. Christensen, *Solid State Commun.* **55**, 351 (1985).
- ⁴²Y. Dou, R. G. Egdell, D. S. L. Law, N. M. Harrison, and B. G. Searle, *J. Phys.: Condens. Matter* **10**, 8447 (1998).
- ⁴³A. Schleife, F. Fuchs, J. Furthmuller, and F. Bechstedt, *Phys. Rev. B* **73**, 245212 (2006).
- ⁴⁴A. Yokozawa and Y. Miyamoto, *Phys. Rev. B* **55**, 13783 (1997).
- ⁴⁵P. E. Blochl and J. H. Stathis, *Phys. Rev. Lett.* **83**, 372 (1999).
- ⁴⁶C. H. Park and D. J. Chadi, *Phys. Rev. Lett.* **84**, 4717 (2000).
- ⁴⁷K. Xiong and J. Robertson, *Appl. Phys. Lett.* **85**, 2577 (2004).
- ⁴⁸J. Robertson, C. W. Chen, W. L. Warren, and C. D. Gutleben, *Appl. Phys. Lett.* **69**, 1704 (1996).
- ⁴⁹S. F. J. Cox, J. L. Gavartin, J. M. Gil, R. C. Vilao, J. S. Lord, and E. A. Davis, *Physica B* **376**, 385 (2006).
- ⁵⁰R. L. Lichti, K. H. Chow, J. M. Gil, D. L. Strpe, R. C. Vilao, and S. F. J. Cox, *Physica B* **376**, 587 (2006).
- ⁵¹P. W. Peacock and J. Robertson, *J. Appl. Phys.* **92**, 4712 (2002).
- ⁵²J. Robertson and B. Falabretti, *J. Appl. Phys.* **100**, 014111 (2006).
- ⁵³D. R. Jennison, P. A. Schultz, and J. P. Sullivan, *Phys. Rev. B* **69**, 041405 (2004).